Facile preparation and electrochemical properties of cubic-phase $Li_4Mn_5O_{12}$ nanowires†

Yang Tian, Dairong Chen,* Xiuling Jiao* and Yongzheng Duan

Received (in Cambridge, UK) 10th January 2007, Accepted 2nd February 2007
First published as an Advance Article on the web 22nd February 2007
DOI: 10.1039/b700385d

Single crystalline $Li_4Mn_5O_{12}$ nanowires with cubic phase were prepared in a large scale by a simple molten salt route without using any surfactant as template; the nanowires exhibited high storage capacity and coulombic efficiency as cathode materials for lithium-ion batteries.

As the cathode materials for rechargeable lithium-ion batteries, lithium manganese oxides (LMO) are of high fundamental and technological interest due to the safety, low cost, and low toxicity of manganese-based compounds.[1] One-dimensional (1D) nanostructured electrode materials have attracted much attention for their higher capacity and stability,[2] which are brought by the limited crystal dimensions and a very high surface-to-bulk ratio.[3] However, although many 1D nanostructured materials including metals, semiconductors and metal oxides have been prepared, there are few reports on the fabrication of 1D LMO nanostructures.[4] This may be due to the complex structural chemistry of the Li–Mn–O system, such as abundant valences of manganese, sensitivity to the temperature and O_2 pressure.[5] Moreover, the preparation of 1D nanostructures of cubic phases are difficult for their isotropic growth in 3D direction, and often need templates (including soft and hard templates),[6] or accessional environmental conditions (such as magnetic field, *etc.*) to assist their fabrication.[7] Thus, it is of importance, but a challenge, to develop simple routes to 1D nanostructures of cubic phase compounds.

The spinel $Li_4Mn_5O_{12}$, having 3D interstitial space for Li^+ cation transport and a theoretical storage capacity of 163 mAh g^{-1} as an electrode material, is one of the most important LMO materials.[1b,8] Here, a molten salt method to the fabrication of $Li_4Mn_5O_{12}$ nanowires is introduced. As a classical route to nanostructured materials, the molten salt method exhibits simplicity and generalizability,[9] and has been applied in large-scale synthesis of 1D nanostructures, in which the surfactant could be used as the template to direct their formation.[10] In the present work, cubic-phase $Li_4Mn_5O_{12}$ nanowires were first prepared without using any template, and the nanowires showed high storage capacity and coulombic efficiency (CE) as cathode materials for lithium-ion batteries.

To prepare the $Li_4Mn_5O_{12}$ nanowires, $MnSO_4$ was added to a mixture of the molten salts $LiNO_3$ and $NaNO_3$ (weight ratio = 1 : 2) at 480 °C under stirring (wt% of $MnSO_4$ in the system was *ca.* 8.5%). After reacting for 10 min, and then cooling to room temperature, the product was obtained by washing the fused material with deionized water several times to remove the nitrates, and dried at 100 °C in air for 12 h.

Fig. 1 shows the powder X-ray diffraction (XRD) pattern of the product, which indicates its high crystallinity. All the peaks can be indexed as the spinel phase of face-centered cubic $Li_4Mn_5O_{12}$ (space group: $Fd\bar{3}m$] without any impurity phase, and the lattice constant a is calculated to be 0.8162 nm based on the XRD data, which is in good agreement with the literature value of 0.8161 nm (JCPDS, No. 46-0810). Transmission electron microscopy (TEM) (Fig. 2(a)) demonstrates that the product consists of uniform nanowires with diameter of 20–30 nm; the length of the nanowires is up to several micrometers leading to a high aspect ratio of ~100, and some of them are slightly bent. The selected area electron diffraction (SAED) pattern (inset of Fig. 2(a)) also illustrates its crystalline nature. Field-emission scanning electron microscopy (FE-SEM, Fig. 2(c)) also confirms their nanowire morphology, and energy dispersive X-ray (EDX) spectroscopy (Fig. 2(d)) shows the element signals of Mn and O without any impurity (such as Na or S), indicating that the product has high chemical purity. The high-resolution TEM (HR-TEM, Fig. 2(b)) image demonstrates the intrinsic crystallography of the as-prepared $Li_4Mn_5O_{12}$ nanowires. The planar spacings of 0.41 and 0.47 nm, corresponding to the spacings of the {002} and {111} planes respectively, indicate the long-axis direction of ⟨110⟩. The fast Fourier transform (FFT) pattern can be indexed to the diffraction pattern of the ⟨110⟩ zone axis of the spinel $Li_4Mn_5O_{12}$, demonstrating the single-crystal nature of the nanowires with the growth direction of ⟨110⟩.

The FT-IR spectrum (see ESI, Fig. S1†) indicates the existence of a few NO_3^- species on the surface of the nanowires besides absorbed water and surface hydroxyls. X-Ray photoelectron spectra (XPS, Fig. 3) analysis gives the binding energy of O 1s and

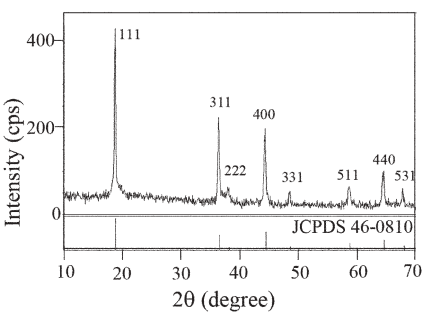

Fig. 1 XRD pattern of the as-prepared $Li_4Mn_5O_{12}$ nanowires.

School of Chemistry and Chemical Engineering, Shandong University, Jinan, 250100, People's Republic of China. E-mail: cdr@sdu.edu.cn; Fax: +86-531-88364281; Tel: +86-531-88364280

† Electronic supplementary information (ESI) available: Experimental details, FT-IR spectra, and XRD patterns of the electrode materials. See DOI: 10.1039/b700385d

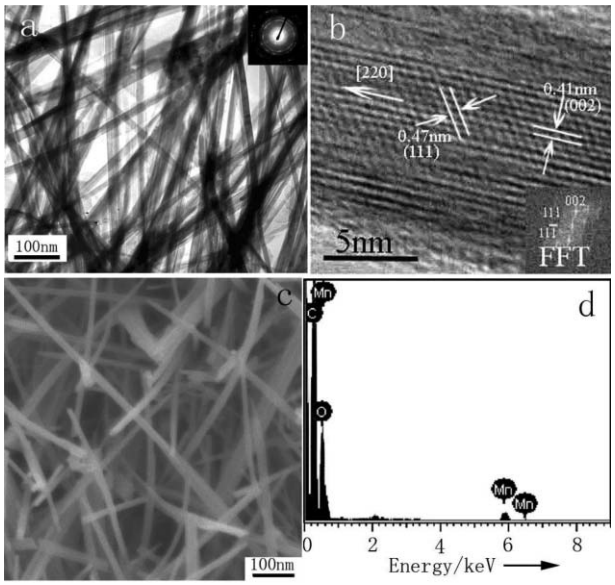

Fig. 2 TEM (a), HR-TEM (b), SEM (c) and EDX (d) images of the as-prepared $Li_4Mn_5O_{12}$ nanowires. The inset in Fig. 2(a) is the corresponding SAED pattern.

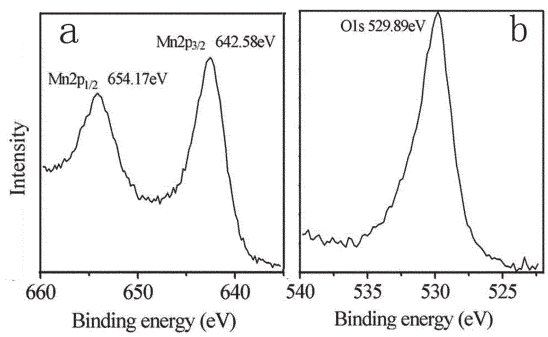

Fig. 3 XPS spectra of Mn (a) and O (b) in the as-prepared $Li_4Mn_5O_{12}$ nanowires.

Mn 2p. The bands at 654.2 and 642.6 eV (Fig. 3(a)) are assigned to the Mn $2p_{1/2}$ and Mn $2p_{3/2}$ binding energies,[11] indicating Mn(IV) state in the product. The band at 529.9 eV (Fig. 3(b)) is attributed to the O 1s binding energy of the crystal lattice oxygen.[12] Although the existence of NO_3^- species can be revealed by the IR spectrum, no bands of N and O atoms from NO_3^- anions can be detected by the XPS technique (owing to its low sensitivity). As to the Li 1s binding energy, only a weak peak is present at *ca.* 55.6 eV due to its small atom sensitive factor (ASF).[13] Based on the peak areas of the Mn $2p_{3/2}$ and O 1s binding energies, the molar ratio of O to Mn is calculated to be *ca.* 2.38, which is close to the theoretical value (2.40) of the spinel $Li_4Mn_5O_{12}$. It is estimated from the result that the molar ratio of Mn(IV) relative to all Mn elements in the product is *ca.* 0.97.

The formation process of the spinel $Li_4Mn_5O_{12}$ was tracked by time-dependent experiments (see ESI, Fig. S2†). The experiments indicated that the product was mainly cubic Mn_2O_3 (JCPDS, No. 78-0390) with a small amount of spinel $Li_4Mn_5O_{12}$ after 30 s of reaction. This was attributed to the thermal decomposition and oxidation of $MnSO_4$ to Mn_2O_3 at temperatures higher than 400 °C. A part of Mn_2O_3 was inserted by Li^+ cations and oxidized to Mn^{4+} to form $Li_4Mn_5O_{12}$. With increased reaction time, the amount of spinel $Li_4Mn_5O_{12}$ increased, and the Mn_2O_3 decreased. After 10 min reaction pure $Li_4Mn_5O_{12}$ was formed. On further prolonging the reaction time no obvious change was observed from the corresponding XRD patterns. Thus it was proposed that the insertion of Li^+ into Mn_2O_3 and the oxidation of Mn^{3+} to Mn^{4+} occurred simultaneously. The reaction took place in two discrete steps: oxidation of Mn^{2+} to Mn^{3+} (eqn (1), fast step) and Li^+ insertion (eqn (2), decisive step). The Mn^{2+} cations were first oxidized to Mn_2O_3 with elimination of NO_2 and O_2, and then the Li^+ cations inserted into Mn_2O_3 to form $Li_4Mn_5O_{12}$, accompanied by oxidation of Mn^{3+} to Mn^{4+}.

$$2Mn^{2+} + 4NO_3^- \rightarrow Mn_2O_3 + 4NO_2 + 1/2O_2 \quad (1)$$

$$5Mn_2O_3 + 8LiNO_3 + 1/2O_2 \rightarrow 2Li_4Mn_5O_{12} + 8NO_2 \quad (2)$$

The morphology evolution of the product during the reaction process was tracked. The results confirm that a lamella-rolling mechanism is reasonable for the formation of $Li_4Mn_5O_{12}$ nanowires. As shown in Fig. 4(a), the product at the initial stage shows the lamellar morphology, and the corresponding SAED pattern (the inset of Fig. 4(a)) illustrates that the product is Mn_2O_3. As the reaction proceeds, the Li^+ cations insert into the crystal lattice of Mn_2O_3 to form $Li_4Mn_5O_{12}$ on the lamellae edges (Fig. 4(b)), and then the lamellae curl to form tubular and wire-like morphologies (Fig. 4(c) and inset). The SAED patterns demonstrate the coexistence of Mn_2O_3 and $Li_4Mn_5O_{12}$ phases at this stage (insets of Fig. 4(b) and (c)). When the reaction time reaches 10 min, all the lamellae transform to the wire-like morphology (Fig. 3(d)) and the SAED pattern illustrates that the product is pure $Li_4Mn_5O_{12}$. It is proposed that the driving force of this transformation is the combined effects of the molten salt medium and insertion of Li^+ cations into Mn_2O_3. The molten salt has strong polarity and high surface tension,[14] and the Mn_2O_3 lamellae with large surface and high surface energy exist in a kinetically metastable state, especially their edges exhibit high activity. Once the $Li_4Mn_5O_{12}$ starts to nucleate along one edge of Mn_2O_3 lamella,

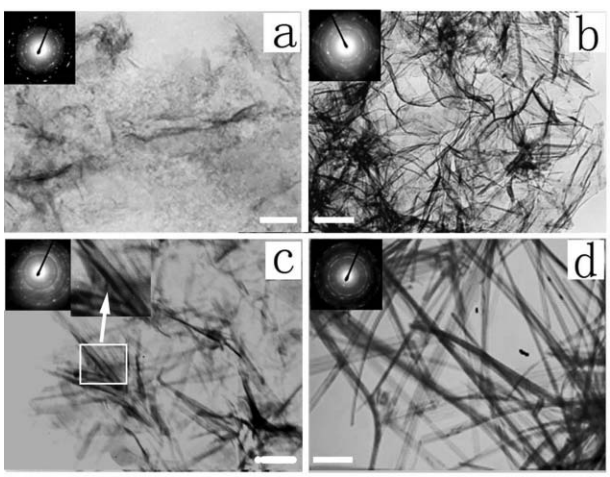

Fig. 4 TEM images of the products with different reaction times: (a) 30 s, (b) 1 min, (c) 3 min, and (d) 10 min. The insets are the corresponding SAED patterns, all the bars are 100 nm.

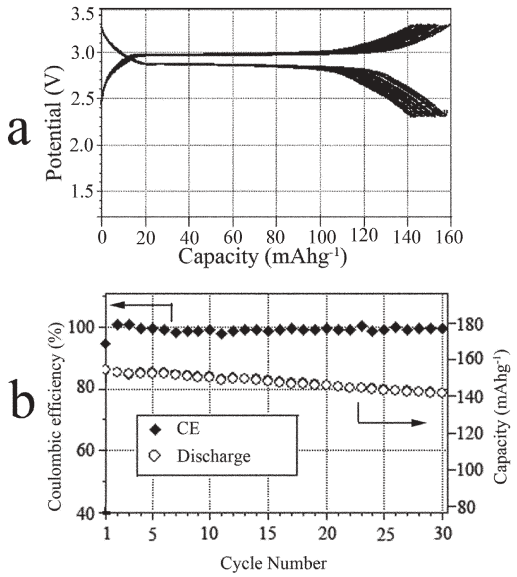

Fig. 5 (a) Charge/discharge curves between 2.3 and 3.3 V. (b) Coulombic efficiency (CE) and discharge capacities as functions of the cycle number at a cycling rate of 0.2 C.

polar interfaces with lower energy than the lamella were formed. To decrease the surface energy, the Mn_2O_3 lamellae would curl and transform into the wire-like morphology. The strong polarity and high tension of the molten salt medium could favor the transformation.

Charging and discharging behaviors of the $Li_4Mn_5O_{12}$ nanowires were studied in an electrochemical half-cell with lithium metal as the counter electrode. The discharge reaction was conducted until a potential of 2.3 V was achieved and the charge reaction was terminated when the potential reached 3.3 V at the discharge/charge rate of 0.2 C. The voltage profiles of the electrochemical cell (Fig. 5(a)) indicate that the working electrode exhibits the typical characteristics of a $Li_4Mn_5O_{12}$ electrode, *i.e.*, a long voltage plateau at $\sim$2.8 V, which is similar to previous reports.[8] During all the cycles, the discharge and charge decrease slightly, demonstrating the high-degree stable discharge plateau at $\sim$2.8 V. Fig. 5(b) shows the cycling behaviors of the $Li_4Mn_5O_{12}$ nanowire electrode for 30 cycles. In the first cycle, the electrode materials have a discharge capacity of 154.3 mAh g^{-1}. Subsequently the discharge capacity decreases slightly but retaining high stability even after 30 cycles. Furthermore, the constructed cell shows highly reversible extraction/insertion of Li into the nanowires, indicating good CE (Fig. 5(b)).[15]

The electrochemical properties of the as-prepared $Li_4Mn_5O_{12}$ nanowires are much improved compared with those of the corresponding bulk and powder materials,[6] which might be attributed to their large surface area, and shorter distance of Li^+ cations grafting in the nanowires. As well known, $Li_4Mn_5O_{12}$ is a stoichiometric spinel ($Li[Li_{0.33}Mn_{1.67}]O_4$) with cubic symmetry, and tends to be converted into the rock salt $Li_{4+x}Mn_5O_{12}$ ($x \leqslant 3$) phase as the Li^+ inserts.[6] The XRD pattern of the working electrode after 30 cycles (see ESI, Fig. S3†) confirmed the structure conversion of the active materials. There are new peaks of (004) and (404) for $Li_{4+x}Mn_5O_{12}$ appearing on the XRD pattern besides the reflections of carbon (JCPDS, No. 26-1080) because of the phase transformation. Comparing the discharge capacity with the theoretical value, x is confirmed to be $\sim$2.6. Based on the XRD data, the lattice parameters are calculated to be a = 0.8104 nm, c = 0.8489 nm, and the volume of the unit cell is 0.5575 nm^3, which expands $\sim$2.54% during the transformation from the cubic (0.5437 nm^3) to the tetragonal phase.[6a]

In summary, we have developed a simple one-pot route of molten salt to high-crystalline spinel $Li_4Mn_5O_{12}$ nanowires in large scale for the first time. The reaction process and formation mechanism of the nanowires were discussed, which is beneficial to the study of 1D nanostructures. As a cathode material for lithium-ion batteries, the as-prepared $Li_4Mn_5O_{12}$ nanowires showed good electrochemical properties, high charge/discharge capacity and high CE.

This work was supported by Program for New Century Excellent Talents in University, P. R. China.

Notes and references

1 (*a*) J.-M. Tarascon and M. Armand, *Nature*, 2001, **414**, 359; (*b*) B. Ammundsen and J. Paulsen, *Adv. Mater.*, 2001, **13**, 943; (*c*) M. Winter, J. O. Besenhard, M. E. Spahr and P. Novák, *Adv. Mater.*, 1998, **10**, 725; (*d*) M. M. Thackeray, C. S. Johnson, J. T. Vaughey, N. Li and S. A. Hackney, *J. Mater. Chem.*, 2005, **15**, 2257.
2 (*a*) G. L. Che, B. B. Lakshmi, E. R. Fisher and C. R. Martin, *Nature*, 1998, **393**, 346; (*b*) R. M, Y. Bando, L. Zhang and T. Sasaki, *Adv. Mater.*, 2004, **16**, 918; (*c*) Y. Gu, D. Chen and X. Jiao, *J. Phys. Chem. B*, 2005, **109**, 17901; (*d*) S. W. Choi, S. M. Jo, W. S. Lee and Y. R. Kim, *Adv. Mater.*, 2003, **15**, 2027; (*e*) M.-S. Wu, P.-C. Chiang, J.-T. Lee and J.-C. Lin, *J. Phys. Chem. B*, 2005, **109**, 23279.
3 (*a*) Y. Xia, P. Yang, Y. Sun, Y. Wu, B. Mayers, B. Gates, Y. Yin, F. Kim and H. Yan, *Adv. Mater.*, 2003, **15**, 353; (*b*) C. Burda, X. Chen, R. Narayanan and M. A. EI-Sayed, *Chem. Rev.*, 2005, **105**, 1025.
4 (*a*) L. Zhang, J. C. Yu, A.-W. Xu, Q. Li, K. W. Kwong and L. Wu, *Chem. Commun.*, 2003, 2910; (*b*) D. H. Park, S. T. Lim, S.-J. Hwang, C.-S. Yoon, Y.-K. Sun and J.-H. Choy, *Adv. Mater.*, 2005, **17**, 2834; (*c*) Y. Tanaka, Q. Zhang and F. Saito, *Powder Technol.*, 2003, **132**, 74; (*d*) S.-H. Kang, J. B. Goodenough and L. K. Rabenberg, *Chem. Mater.*, 2001, **13**, 1758.
5 (*a*) P. Piszora, *Chem. Mater.*, 2006, **18**, 4802; (*b*) J. M. Paulsen and J. R. Dahn, *Chem. Mater.*, 1999, **11**, 3065.
6 See, for example: (*a*) Y. Sun and Y. Xia, *Adv. Mater.*, 2002, **14**, 833; (*b*) J. J. Urban, W. S. Yun, Q. Gu and H. Park, *J. Am. Chem. Soc.*, 2002, **124**, 1186; (*c*) M. E. T. Molares, V. Buschmann, D. Dobrev, R. Neumann, R. Scholz, I. U. Schuchert and J. Vetter, *Adv. Mater.*, 2001, **13**, 62.
7 (*a*) J. Wang, Q. Chen, C. Zeng and B. Hou, *Adv. Mater.*, 2004, **16**, 137.
8 (*a*) M. M. Thackeray, A. Kock, M. H. Rossouw, D. Liles, R. Bittihn and D. Hoge, *J. Electrochem. Soc.*, 1992, **139**, 363; (*b*) T. Takada, H. Hayakawa, E. Akiba, F. Izumi and B. C. Chakoumakos, *J. Power Sources*, 1997, **68**, 613; (*c*) J. Kim and A. Manthiram, *J. Electrochem. Soc.*, 1998, **145**, L53.
9 (*a*) Y. Mao and S. S. Wong, *Adv. Mater.*, 2005, **17**, 2194; (*b*) Y. Tian, D. Chen and X. Jiao, *Chem. Mater.*, 2006, **18**, 6088; (*c*) M. J. Geselbracht, L. D. Noailles, L. T. Ngo, J. H. Pikul, R. I. Walton, E. S. Cowell, F. Millange and D. O'Hare, *Chem. Mater.*, 2004, **16**, 1153.
10 Y. Mao, S. Banerjee and S. S. Wong, *J. Am. Chem. Soc.*, 2003, **125**, 15718.
11 F. A. Al-Sagheer and M. I. Zaki, *Colloids Surf., A*, 2000, **10**, 193.
12 M. Manickam, P. Singh, T. B. Issa, S. Thurgate and R. D. Marco, *J. Power Sources*, 2004, **130**, 254.
13 C. D. Wang, J. F. Moulder, L. E. Davis and W. M. Riggs, Perkin-Elmer Corporation, Physical Electronics Division (end of book).
14 I. Krossing, J. M. Slattery, C. Daguenet, P. J. Dyson, A. Oleinikova and H. Weingartner, *J. Am. Chem. Soc.*, 2006, **128**, 13427.
15 S.-H. Ng, J. Wang, D. Wexler, K. Konstantinov, Z.-P. Guo and K. Liu, *Angew. Chem., Int. Ed.*, 2006, **45**, 6896.

